



## OPEN

## SUBJECT AREAS:

ENVIRONMENTAL  
SCIENCES

BIOGEOCHEMISTRY

POLLUTION REMEDIATION

FOREST ECOLOGY

Received  
16 April 2013Accepted  
13 August 2013Published  
2 September 2013Correspondence and  
requests for materials  
should be addressed to  
S.H. (shojih@ffpri.  
affrc.go.jp)

# Predicted spatio-temporal dynamics of radiocesium deposited onto forests following the Fukushima nuclear accident

Shoji Hashimoto<sup>1</sup>, Toshiya Matsuura<sup>2</sup>, Kazuki Nanko<sup>1</sup>, Igor Linkov<sup>3</sup>, George Shaw<sup>4</sup> & Shinji Kaneko<sup>1</sup>

<sup>1</sup>Department of Forest Site Environment, Forestry and Forest Products Research Institute (FFPRI), 1 Matsunosato, Tsukuba, Ibaraki, 305-8687, Japan, <sup>2</sup>Department of Forest Management, Forestry and Forest Products Research Institute (FFPRI), 1 Matsunosato, Tsukuba, Ibaraki, 305-8687, Japan, <sup>3</sup>US Army Engineer Research and Development Center, 3909 Halls Ferry Road, Vicksburg, MS, 39180-6199, USA, <sup>4</sup>School of Biosciences, University of Nottingham, Sutton Bonington Campus, Sutton Bonington, Leicestershire, LE12-5RD, UK.

The majority of the area contaminated by the Fukushima Dai-ichi nuclear power plant accident is covered by forest. To facilitate effective countermeasure strategies to mitigate forest contamination, we simulated the spatio-temporal dynamics of radiocesium deposited into Japanese forest ecosystems in 2011 using a model that was developed after the Chernobyl accident in 1986. The simulation revealed that the radiocesium inventories in tree and soil surface organic layer components drop rapidly during the first two years after the fallout. Over a period of one to two years, the radiocesium is predicted to move from the tree and surface organic soil to the mineral soil, which eventually becomes the largest radiocesium reservoir within forest ecosystems. Although the uncertainty of our simulations should be considered, the results provide a basis for understanding and anticipating the future dynamics of radiocesium in Japanese forests following the Fukushima accident.

The accident at the Fukushima Dai-ichi nuclear power plant (FDNPP) resulted from the Great East Japan Earthquake of 11<sup>th</sup> March, 2011. This earthquake caused a tsunami of unprecedented magnitude that flooded and disabled cooling systems at the power plant, leading to catastrophic releases of radionuclides into the environment. The main radionuclides released into the atmosphere were iodine (<sup>131</sup>I, half-life 8 days) and cesium (<sup>134</sup>Cs, half-life 2 years, and <sup>137</sup>Cs, half-life 30 years), which were deposited over a large area of Japan's land surface<sup>1-4</sup>. Because of their longer half-lives, tracking and forecasting the behaviour and impacts of <sup>134</sup>Cs and <sup>137</sup>Cs are priorities<sup>5</sup>; in particular, the <sup>137</sup>Cs environmental contamination is expected to persist for decades.

The majority of the contaminated area (approximately 70%) is covered by forests<sup>6</sup>. According to studies conducted in the forests contaminated by the Chernobyl accident<sup>7-10</sup>, the radiocesium deposited from the atmosphere onto forest canopies subsequently migrates between the structural components of the forest ecosystem, including the aboveground tree components (leaves/needles and branches), soil litter and surface organic layers, and the underlying mineral soil. The radiocesium in the atmosphere is first deposited on leaves/needles, branches, bark, and the soil surface organic layer (forest floor litter). This deposited radiocesium, primarily within the tree canopy, is then transferred to the soil surface via rainfall and with the shedding of dead leaves/needles and branches from the tree to the forest floor<sup>11-15</sup>. Over the longer term, radiocesium in the surface organic layers on the forest floor moves into the mineral soil, while some of the radiocesium in organic and mineral soil layers is absorbed by plant roots and transferred into aboveground plant organs. In broad terms, although a portion of the deposited radiocesium might migrate from forests via stream flow, forest ecosystems provide effective reservoirs for radiocesium and do not tend to discharge the radiocesium substantially in the long term.

To develop effective countermeasures to mitigate the impacts of radioactive contamination of forests, detailed monitoring of the radiocesium migration and re-distribution is essential. In addition, it is useful to be able to predict the future dynamics of the radiocesium between forest components; modelling is the best tool for this prediction<sup>16-19</sup>.

Here, we report the simulated dynamics of the radiocesium deposited in forests in Japan using a model for radionuclides in a forest ecosystem (RIFE1 model)<sup>8,16,18</sup>. Model simulations were run using initial conditions based on the observed radiocesium distributions among the structural components of forests contaminated by the Fukushima fallout. We have simulated the radiocesium dynamics in evergreen needleleaf forests and deciduous



broadleaf forests over a period of 20 years from the initial contamination. Furthermore, we have combined the simulation results with spatial data from an airborne radionuclide survey to forecast the radiocesium dynamics in forest ecosystems both spatially and temporally.

## Results

The time courses of  $^{137}\text{Cs}$  and  $^{134}\text{Cs}$  within each forest component are shown in Figure 1. As expected from the different half-lives of  $^{137}\text{Cs}$  and  $^{134}\text{Cs}$ , the total  $^{137}\text{Cs}$  activity decreases quite slowly compared to that of  $^{134}\text{Cs}$  (Fig. 1AD for  $^{137}\text{Cs}$  and Fig. 1BE for  $^{134}\text{Cs}$ ). The total  $^{134}\text{Cs}$  inventory was almost equivalent to  $^{137}\text{Cs}$  at the time of initial deposition (year 0) but will become less than 10% of the total initial inventory after 5 years. The total  $^{137}\text{Cs}$  and  $^{134}\text{Cs}$  combined inventory drops rapidly after the fallout and will decrease to approximately half of the initial fallout after approximately 10 years, primarily because of the radioactive decay of  $^{134}\text{Cs}$  (Fig. 1CF). However, the rate at which the total radiocesium inventory decreases will slow after 10 years, when  $^{137}\text{Cs}$  remains as the dominant nuclide.

As for the total radiocesium in each component, very similar trends are observed in both forest types (Fig. 1CF). First, the total radiocesium inventory in tree components drops rapidly during the first two years after the fallout. The radiocesium in the soil surface organic layer also decreases exponentially with time. In contrast, the inventory within the mineral soil compartment peaks during the first year (Fig. 1F, deciduous broadleaf forests) or second year (Fig. 1C, evergreen needleleaf forests) and then decreases slowly, primarily because of radioactive decay. Because of its shorter half-life, the  $^{134}\text{Cs}$  inventory in the mineral soil compartment starts decreasing approximately one year after the initial fallout (Fig. 1BE). The  $^{137}\text{Cs}$  inventory in the mineral soil compartment peaks during the fifth/sixth year (Fig. 1AD).

Coupling the modelling results with an airborne gamma activity survey map enabled us to predict the spatio-temporal evolution of the total radiocesium inventory in forest ecosystems (Fig. 2 and Supplementary Movie S1). The top row images in Figure 2 show the diminishing extent of the contaminated areas due to the physical decay of radiocesium over a 20 year period. For example, comparing the map of year 0 with the distribution after 20 years, the highly

contaminated areas (yellow and red areas) located northwest of the FDNPP clearly decrease, and the blue areas, which are of relatively low contamination, are substantially diminished in size. The lower three rows show the radiocesium migration between forest components and the overall reduction in activity due to the physical decay of  $^{137}\text{Cs}$  and  $^{134}\text{Cs}$ . The radiocesium in trees and in the soil surface organic layer is clearly visible at the time the fallout occurred, but the contamination decreases rapidly, resulting in a transfer of radioactivity to the mineral soil during the first two years after the fallout. In contrast, the mineral soil contamination becomes the largest radiocesium reservoir in the second year. The mineral soil radiocesium inventory does not decrease significantly as a result of the balance between the decrease in the amount of radiocesium due to physical decay and its migration from the soil surface organic layer above the mineral soil during the early stage, and because of the longer half-life of  $^{137}\text{Cs}$ .

## Discussion

In European forests contaminated by the Chernobyl accident, the organic soil layer retained the largest portion of radiocesium and thus played a critical role in controlling radiocesium migration in forest ecosystems<sup>7,17,20</sup>. However, the data obtained from our study sites in the Fukushima prefecture indicate that the majority of radiocesium had already migrated to the mineral soil layer in 2012, thus demonstrating that the migration through the organic soil layer is more rapid than in European forests contaminated by fallout from Chernobyl. This is one of important radioecological differences between Fukushima and Chernobyl<sup>7,17,20</sup>. Our modelling study is not designed to reveal the underlying mechanisms of this fast migration, and therefore further observation studies and analysis of physicochemical properties of forest soils in Fukushima must be continued. However, we hypothesize that this fast migration is a result of the relatively warm climate and heavy rainfall which lead to more rapid litter decomposition and substantially thinner organic soil layers than in many European forests (see below).

Our simulations demonstrate the time courses of the total radiocesium inventories and the individual radionuclides ( $^{137}\text{Cs}$  and  $^{134}\text{Cs}$ ) in evergreen needleleaf and deciduous broadleaf forests. The results showed that, without decontamination, the total inventory will

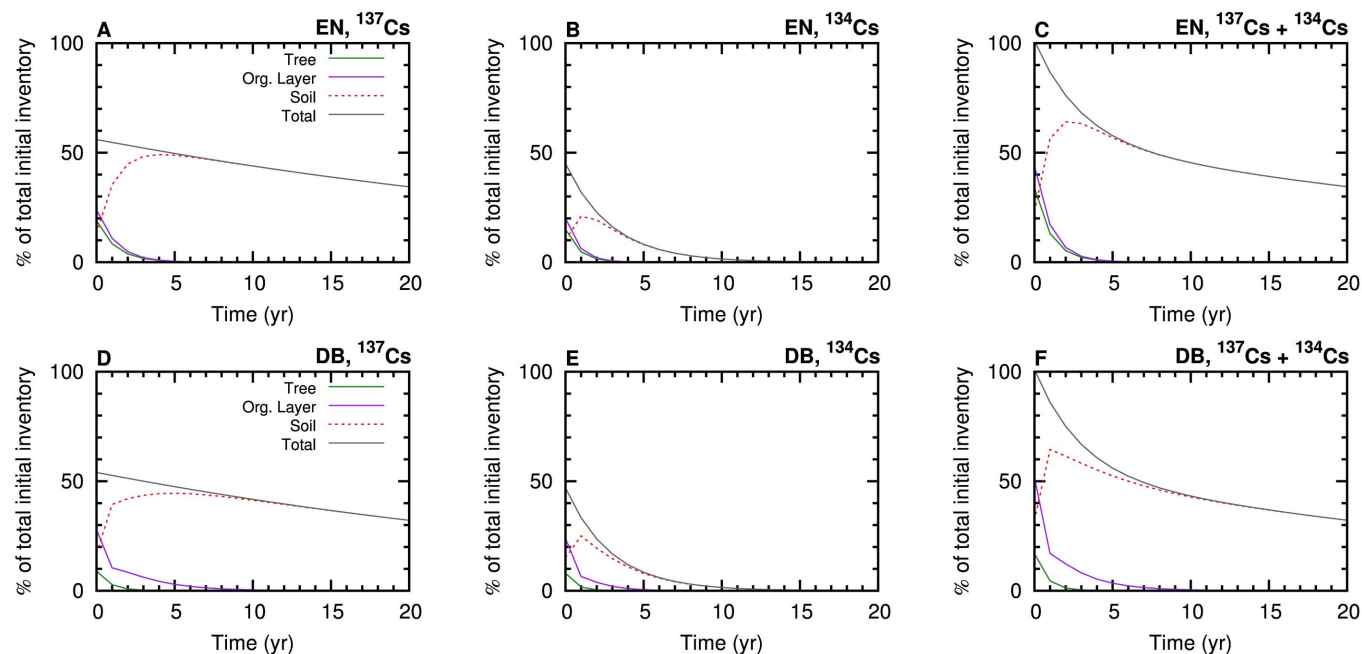


**Figure 1** | Time courses of  $^{137}\text{Cs}$ ,  $^{134}\text{Cs}$ , and total radiocesium ( $^{137}\text{Cs} + ^{134}\text{Cs}$ ). Evergreen needleleaf forests (EN, above) and deciduous broadleaf forests (BD, below). The redistribution of the total initial inventory was simulated on a percentage basis.

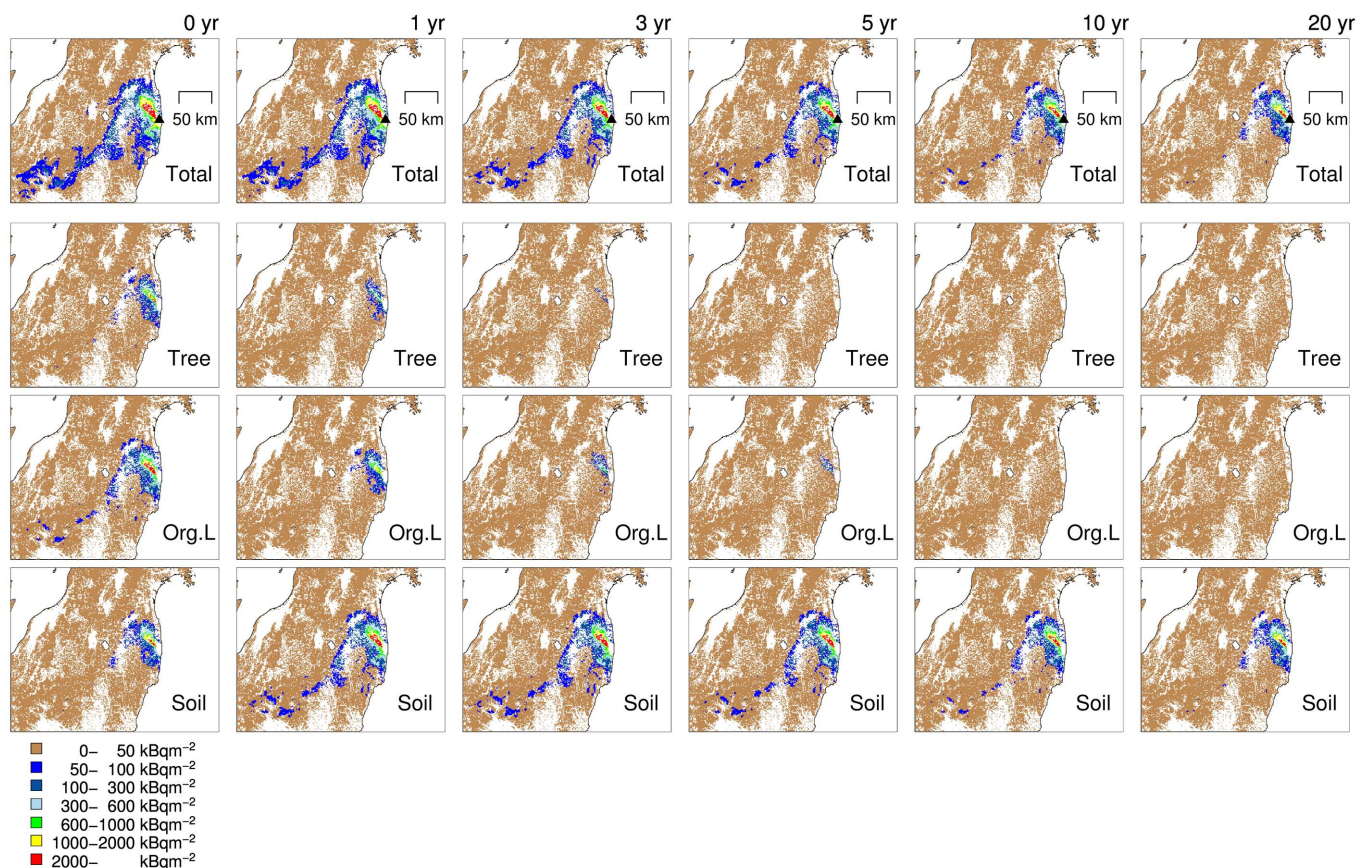


**Figure 2 | Predicted spatio-temporal distributions of the radiocesium deposited into forests.** The results at 0, 1, 3, 5, 10, and 20 years after the accident are shown from left to right. The upper row shows the total radiocesium in forest ecosystems; the second, third, and fourth rows show the radiocesium in tree (Tree), soil surface organic layer (Org.L), and mineral soil (Soil) components, respectively. The black triangle indicates the location of Fukushima Dai-ichi nuclear power plant (FDNPP). White areas are not covered by forests. The spatial radiocesium distribution map we obtained did not include the area near the FDNPP. The maps were created using the Generic Mapping Tools (GMT)<sup>29</sup>.

decrease to approximately 50% of the total initial inventory in 5–10 years after the fallout due to the radioactive decay of  $^{134}\text{Cs}$  and that, after 5–10 years, the mineral soil compartment will retain most of the radiocesium (mostly  $^{137}\text{Cs}$  at  $> 5$  years). Furthermore, the simulation results provide guidance for the design of effective forest ecosystem decontamination strategies<sup>21</sup>. First, despite the different radiocesium distributions in the two forest types at the time of fallout, the overall trends of the contamination inventories were the same in both evergreen needleleaf forests and deciduous broadleaf forests. Second, it is clear that removing tree components is not an effective means of removing the radiocesium from the ecosystems unless it is performed shortly after the fallout. Our simulation results suggest that the radiocesium within the tree component decreases rapidly within the first two years. Third, removing the soil surface organic layer would be effective during a period of approximately two years after the fallout, but the effectiveness of this countermeasure decreases rapidly after this time.

Another conclusion that can be drawn from our simulation is that the risk of radiocesium migration from forest ecosystems to adjacent land areas will decrease rapidly during the first two years because migration occurs from the soil surface organic layer into the mineral soil compartment, which is much less likely to be subject to lateral transport by wind or water. The soil surface organic layer is more susceptible to physical redistribution by erosion than the mineral soil, and furthermore, the radiocesium in mineral soils can be strongly fixed in mineral particles and is, thus, chemically less mobile<sup>18,19</sup>.

The forests in Japan experience high mean annual precipitation (approximately 1500 mm; area of  $\geq 137$ ,  $^{134}\text{Cs}$  50 kBq  $\text{m}^{-2}$  in September 2011) with occasional heavy rainfall from typhoons and the monsoon. This precipitation, coupled with a warm climate (mean annual temperature, approximately 10°C), will most likely increase the rate of radiocesium circulation within forest ecosystems. In particular, it is possible that high and intense rainfall and rapid decomposition of organic matter within the soil surface organic layer will combine to accelerate radiocesium migration from the soil surface organic layer to the mineral soil.

A possibly accelerated rate of radiocesium migration in Japanese soil surface organic layers was included in our simulations by assuming reduced thicknesses of the layers compared with those reported in the Chernobyl studies, and also by shorter residence half-lives for radiocesium within the organic soil layer ( $k_6$ ) (see Methods and Supplementary Table S1). These results imply that forest decontamination by removing contaminated aboveground components (e.g., leaves, tree boles, branches, and soil surface organic layers) should be performed more rapidly than expected based on the experience of Chernobyl<sup>21</sup>. In the worst case, it might already be too late to remove the bulk of the forest contamination by removing the aboveground components, and probably the mineral soil must be removed to achieve effective decontamination. However, removing the mineral soil will incur significantly greater cost than removing the aboveground components. Furthermore, it should be noted that large scale removal of trees and soils may increase soil erosion and landslides, and will also result in reduction of biodiversity and degradation of



soil nutrient and water retention functions. Therefore, the feasibility of removal of contaminated materials from large areas needs to be evaluated by cost-benefit analysis. More optimistically, the rapid radiocesium migration to mineral soil components may indicate an equal reduction in the physico-chemical mobility of radiocesium in forest ecosystems. The radiocesium in mineral soil components, especially clay minerals, is the most stable and recalcitrant form of radiocesium in the environment.

In this study, the time courses of radiocesium in forests were simulated using the RIFE1 model. Although the uncertainties in our simulations should be considered, our results support the idea that selective countermeasure strategies can be developed to reduce forest contamination. There is a wide range of different countermeasure options which have previously been proposed<sup>7,22–25</sup> and each of these should be examined and tested carefully before application. Specifically, the potential for reduction of radiation dose, the feasibility and cost, the possible ecological effects, and the social acceptability of each countermeasure should be taken into account before it can be applied<sup>7,22–25</sup>. In reality, the availability of countermeasure options for forest areas is limited to the restriction of access and removal of contaminated materials, and both of these options have their advantages and disadvantages<sup>7,22–25</sup>. Therefore, a combination of the above two options (zoning) could provide a realistic and balanced approach to the management of contaminated forests. Data revealing the radiocesium dynamics in Japanese forests are limited. At the time of writing, less than three years after the Fukushima accident, data are not necessarily sufficient fully to parameterise models of radionuclide dynamic for longer-term predictions. However, the model used in this study was widely tested against data observed in forests contaminated by the Chernobyl accident, and we carefully parameterised and tested the model using data observed in the Fukushima area as fully as possible at this stage. Moreover, to develop effective countermeasures at an early stage, anticipation of the future dynamics of radiocesium in forest ecosystems is urgently required. We acknowledge that continued monitoring is necessary, together with iterative model parameterisation and validation in future years. Nevertheless, our simulation results at this early stage will assist in understanding and anticipating the future dynamics of radiocesium in Japanese forests.

## Methods

The RIFE1 (Radionuclides in Forest Ecosystems) model was used in this study. The RIFE1 model was developed by Shaw and Belli<sup>8,16,18</sup> after the Chernobyl accident to track the radionuclide dynamics in forest ecosystems and has been tested and calibrated using the data from eight forest sites in Europe<sup>18,19</sup>. RIFE1 is one of the models tested in a model inter-comparison programme of International Atomic Energy Agency<sup>16,19</sup>. RIFE1 is a relatively simple dynamic compartment model of radionuclide redistribution following a single deposition event and is designed to provide forecasts of the radionuclide dynamics in forest ecosystems to help develop decision making strategies following forest contamination (Supplementary Fig. S1). The model consists of five compartments (tree external, tree internal, litter, organic soil, and mineral soil), and these pools are linked by radionuclide fluxes (Supplementary Fig. S1). Each flux is described as a first-order rate process, which can be represented by a time-invariant rate coefficient. The model equations are as follows:

$$dQ_1/dt = I_1 - (k_1 + k_4 + \lambda)Q_1$$

$$dQ_2/dt = k_1Q_1 + k_3Q_4 - (k_2 + \lambda)Q_2$$

$$dQ_3/dt = I_2 + k_4Q_1 + k_2Q_2 - (k_5 + \lambda)Q_3$$

$$dQ_4/dt = k_5Q_3 - (k_3 + k_6 + \lambda)Q_4$$

$$dQ_5/dt = k_6Q_4 - (k_7 + \lambda)Q_5$$

where  $Q_1$ ,  $Q_2$ ,  $Q_3$ ,  $Q_4$ , and  $Q_5$  are the activity inventories of a radionuclide within the tree external, tree internal, litter (fresh dead leaves on the soil surface), soil surface organic soil (decomposed organic matter on the soil surface; F and H layers combined), and mineral soil components, respectively ( $\text{Bq m}^{-2}$ ).  $k_1$  is the rate coefficient of radionuclide transfer between compartments ( $\text{yr}^{-1}$ ), and  $\lambda$  is the rate constant of radioactive decay ( $\text{yr}^{-1}$ ) for the radionuclide being considered.  $t$  is the time (yr), and  $I_1$

and  $I_2$  are the inputs of radionuclides to the tree external and litter components, respectively. The residence half-lives ( $T_h$ , yr) used in this study are shown in Supplementary Table S1. The  $^{137}\text{Cs}$  and  $^{134}\text{Cs}$  dynamics were simulated in this study. The half-lives were converted into the appropriate rate coefficients using the following relationship.

$$k \text{ (or } \lambda) = \ln(2)/T_h$$

Because it is difficult to estimate the leaf absorption parameter ( $k_1$ ), the rate was set to zero, as in the original study. The values for  $k_5$ ,  $k_6$ , and  $k_7$  were multiplied by the thickness of the layer when used.

We used the inventories of radiocesium ( $^{137}\text{Cs}$ ,  $^{134}\text{Cs}$ ) measured in September 2011 in Otama village ( $37^\circ 34' \text{N}$ ,  $140^\circ 18' \text{E}$ ) in the Fukushima prefecture as the initial conditions for this simulation<sup>26</sup> (the location of the FDNPP is shown in Supplementary Fig. S2). The two most common forest types were included: evergreen needleleaf forest (mainly *Cryptomeria japonica*) and deciduous broadleaf forest (mainly *Quercus serrata*). The observed  $^{137}\text{Cs}$  and  $^{134}\text{Cs}$  distributions as percentages of the total inventory (i.e.,  $^{137}\text{Cs} + ^{134}\text{Cs}$ ) were used as the initial conditions (Supplementary Table S2); hence, we simulated the radiocesium redistribution on a percentage basis. The major difference in the radiocesium inventory between evergreen needleleaf forests and deciduous broadleaf forests was that the contribution of the litter component was low for evergreen needleleaf forests and high for deciduous broadleaf forest, most likely because the trees in the deciduous forests were at a stage prior to leaf growth when the radioactive materials were discharged. The depth of the litter and organic soil for  $k_5$  and  $k_6$  were set to 0.017 and 0.012 m ( $N = 88$ ), respectively, which were measured in Fukushima in the national soil carbon inventory project. In the field measurement data obtained, the portions of radiocesium in the litter and organic soil were not distinguished; we assumed that 20% of the observed radiocesium was retained in the litter (L layer) and that 80% was in the organic soil (F and H layers). Because our field observation monitors the mineral soil layer over a depth of 0–0.2 m, we set the mineral soil layer thickness at 0.2 m for  $k_7$ . In this study, we simulated the dynamics of  $^{137}\text{Cs}$ ,  $^{134}\text{Cs}$ , and the total radiocesium in the tree components ( $Q_1 + Q_2$ , Tree external and Tree internal in RIFE 1), soil surface organic layer ( $Q_3 + Q_4$ , Litter and organic soil in the model), and mineral soil ( $Q_5$ , Mineral soil in the model). The time courses of each raw component from the model are shown in Supplementary Figure S3. The transfers to understory vegetation and mushrooms were calculated using transfer factors in the RIFE1 model, but these transfers were not included in this simulation. Monthly time steps were adopted in the simulation.

The model was parameterised using the data observed in the first and second years after the Fukushima accident<sup>26</sup>. A Bayesian calibration scheme, which is an optimization scheme that uses Monte Carlo sampling, was used to estimate the best parameter sets ( $k_2$ – $k_7$ ) and their uncertainty ranges (Supplementary Table S1). Details about the Bayesian calibration scheme are described elsewhere<sup>27</sup>. We conducted 100000 iterations of sampling, and discarded the first 20000 iterations as burn-in to avoid the influence of the initial values. Using the original parameter set (geometric means of eight sites in Europe) the model overestimated the % of total radiocesium inventory in the soil surface organic layer and underestimated that in the mineral soil (Fig. S4). After the parameterisation, however, the model accurately reproduced the distribution of radiocesium in forest ecosystems one year after the fallout (Fig. S4). Because of the limited data, the parameters have large uncertainty ranges.

The simulated results were validated by comparing estimated percentages of total radiocesium inventory in the second year with observed data at four needleleaf forest sites (Fig. S5 and Table S3) (ref. 26). The data used for validation were not used for model parameterisation. The inventories of radiocesium in tree external ( $E_{1,2,3,4}$ ), tree internal ( $I_{1,2,3,4}$ ), soil surface organic layer ( $O_{1,2,3,4}$ ), and mineral soil ( $S_{1,2,3,4}$ ) components were compared. The data were obtained in Kawauchi village ( $E_1$ ,  $I_1$ ,  $O_1$ ,  $S_1$ , and  $E_4$ ,  $I_4$ ,  $O_4$ ,  $S_4$ ), Otama village ( $E_2$ ,  $I_2$ ,  $O_2$ ,  $S_2$ ), and Tadami town ( $E_3$ ,  $I_3$ ,  $O_3$ ,  $S_3$ ) (Table S3) (ref. 26). Overall, the simulation results were well correlated with observed data, showing high radiocesium inventories in mineral soil components and low inventories in tree and soil surface organic layers. However, relatively larger discrepancies between simulated and observed values were found for site 4 ( $E_4$ ,  $O_4$ ,  $S_4$ ), where larger leaf and branch biomass and a thicker soil surface organic layer than other sites were reported<sup>26</sup>. These validations suggest that overall dynamics of radiocesium in Japanese forests were similar, and the RIFE1 model can accurately capture the overall dynamics of radiocesium in Japanese forests. However, since the dynamics of radiocesium in forests differ depending on forest conditions (e.g. tree biomass and soil surface organic layer), specific parameterisation would be needed for forests with distinctly different characteristics from the 'typical' forests of the Fukushima region. Also we emphasise that monitoring, together with iterative model parameterisation and validation, must be continued in future years.

We combined the simulation results with a spatial radiocesium distribution map that was measured by an air-borne radiometric survey<sup>1,2</sup>. The map we obtained did not include the area near the FDNPP. We converted the map into a grid of 1 km squares and then extracted data from the areas containing forest. The evergreen needleleaf forest and deciduous broadleaf forests were distinguished using a vegetation database<sup>28</sup>. We multiplied the total radiocesium in a grid, as estimated by the air-borne survey ( $T_{RC}$ ,  $\text{kBq m}^{-2}$ ), with our simulation results (e.g.,  $^{134}\text{Q}_5, t = 3$ , the  $^{134}\text{Cs}$  in the mineral soil component 3 years after the fallout, as a proportion of the total initial deposition, %) and estimated the radiocesium dynamics in each grid. For example, the  $^{134}\text{Cs}$  inventory in the mineral soil compartment 3 years after the fallout ( $\text{kBq m}^{-2}$ ) can be calculated as  $T_{RC} \times ^{134}\text{Q}_5, t = 3/100$  (e.g.,  $10.0 \text{ kBq m}^{-2} \times 30\%/100 = 3.0 \text{ kBq m}^{-2}$ ).



The dominant forest types in the contaminated area are evergreen needleleaf forests and deciduous broadleaf forests. The flora in Japanese forests is rich and diverse. The dominant tree species in evergreen needleleaf forests are *Cryptomeria japonica* (Japanese cedar) and *Chamaecyparis obtusa* (Japanese cypress), and those in deciduous broadleaf forests are *Fagus japonica*, *Fagus crenata*, *Quercus serrata*, and *Quercus crispula*. Brown forest soils (Cambisols and Andosols in the classification of the Food and Agriculture Organization) are distributed most widely in the area (approximately 70%), and Black soils (Andosols) are also present (approximately 20%).

- Japanese Ministry of Education, Culture, Sports, Science, and Technology: *Detailed Distribution Map of Radiation Dose/Cyber National Land* <<http://ramap.jmc.or.jp/map/eng/>> (accessed 13 June 2013).
- Japanese Ministry of Education, Culture, Sports, Science, and Technology: *Results of the Fourth Airborne Monitoring Survey by MEXT* <[http://radioactivity.nsr.go.jp/en/contents/4000/3179/24/1270\\_1216.pdf](http://radioactivity.nsr.go.jp/en/contents/4000/3179/24/1270_1216.pdf)> (accessed 13 June 2013).
- Kinoshita, N. *et al.* Assessment of individual radionuclide distributions from the Fukushima nuclear accident covering central-east Japan. *Proc. Natl. Acad. Sci. USA* **108**, 19526–19529 (2011).
- Yasunari, T. J. *et al.* Cesium-137 deposition and contamination of Japanese soils due to the Fukushima nuclear accident. *Proc. Natl. Acad. Sci. USA* **108**, 19530–19534 (2011).
- Yoshida, N. & Kanda, J. Tracking the Fukushima radionuclides. *Science* **336**, 1115–1116 (2012).
- Hashimoto, S., Ugawa, S., Nanko, K. & Shichi, K. The total amounts of radioactively contaminated materials in forests in Fukushima, Japan. *Sci. Rep.* **2**, 416 (2012).
- International Atomic Energy Agency: *Environmental Consequences of the Chernobyl Accident and their Remediation: Twenty Years of Experience* <[http://www-pub.iaea.org/mtcd/publications/pdf/pub1239\\_web.pdf](http://www-pub.iaea.org/mtcd/publications/pdf/pub1239_web.pdf)> (accessed 13 June 2013).
- Linkov, I. & Schell, W. R. ed.: *Contaminated Forests: Recent Developments in Risk Identification and Future Perspectives*. (Kluwer Academic Publishers, 1999).
- Tikhomirov, F. A. & Shcheglov, A. I. Main investigation results on the forest radioecology in the Kyshtym and Chernobyl accident zones. *Sci. Total Environ.* **157**, 45–57 (1994).
- Shaw, G. in *Radioactivity in the terrestrial environment: Radionuclides in forest ecosystems* (ed. Shaw, G.) 127–156 (Elsevier, 2007).
- Tagami, K., Uchida, S., Ishii, N. & Kagiya, S. Translocation of radiocesium from stems and leaves of plants and the effect on radiocesium concentrations in newly emerged plant tissues. *J. Environ. Radioact.* **111**, 65–69 (2012).
- Kato, H., Onda, Y. & Gomi, T. Interception of the Fukushima reactor accident-derived <sup>137</sup>Cs, <sup>134</sup>Cs and <sup>131</sup>I by coniferous forest canopies. *Geophys. Res. Lett.* **39**, L20403 (2012).
- Koarashi, J. *et al.* Retention of potentially mobile radiocesium in forest surface soils affected by the Fukushima nuclear accident. *Sci. Rep.* **2**, 1005 (2012).
- Koarashi, J. *et al.* Factors affecting vertical distribution of Fukushima accident-derived radiocesium in soil under different land-use conditions. *Sci. Total Environ.* **431**, 391–401 (2012).
- Yoshihara, T., Matsumura, T., Hashida, S. & Nagaoka, T. Radiocesium contaminations of 20 wood species and the corresponding gamma-ray dose rates around the canopies at 5 months after the Fukushima nuclear power plant accident. *J. Environ. Radioact.* **115**, 60–68 (2013).
- International Atomic Energy Agency: *Modelling the Migration and Accumulation of Radionuclides in Forest Ecosystems*. Report of the Forest Working Group of the Biosphere Modelling and Assessment (BIOMASS) Programme (Theme 3) <[http://www-pub.iaea.org/MTCD/publications/PDF/Biomass1\\_web.pdf](http://www-pub.iaea.org/MTCD/publications/PDF/Biomass1_web.pdf)> (accessed 13 June 2013).
- Shcheglov, A. I., Tsvetnova, O. B. & Klyashtorin, A. L. *Biogeochemical Migration of Technogenic Radionuclides in Forest Ecosystems* (Nauka, 2001).
- Belli, M. ed.: *SEMINAT—Radionuclides in Semi-Natural Environments, Final report 1996–1999* –EC Research Contract n°F14P-CT95-0022 (2000).
- Shaw, G. *et al.* Radionuclide migration in forest ecosystems – results of a model validation study. *J. Environ. Radioact.* **84**, 285–296 (2005).
- Fesenko, S. V. *et al.* Identification of processes governing long-term accumulation of <sup>137</sup>Cs by forest trees following the Chernobyl accident. *Radiat. Environ. Biophys.* **40**, 105–113 (2001).
- Linkov, I., Morel, B. & Schell, W. R. Remedial policies in radiologically-contaminated forests: environmental consequences and risk assessment. *Risk Anal.* **17**, 67–75 (1997).
- Fesenko, S. V., Voigt, G., Spiridonov, S. I. & Gontarenko, I. A. Decision making framework for application of forest countermeasures in the long term after the Chernobyl accident. *J. Environ. Radioact.* **82**, 143–166 (2005).
- Guillitte, O. & Willdrodt, C. An assessment of experimental and potential countermeasures to reduce radionuclide transfers in forest ecosystems. *Sci. Total Environ.* **137**, 273–288 (1993).
- Guillitte, O., Tikhomirov, F. A., Shaw, G. & Vetrov, V. Principles and practices of countermeasures to be carried out following radioactive contamination of forest areas. *Sci. Total Environ.* **157**, 399–406 (1994).
- Hashimoto, S., Linkov, I., Shaw, G. & Kaneko, S. Radioactive contamination of natural ecosystems: seeing the wood despite the trees. *Environ. Sci. Tech.* **46**, 12283–12284 (2012).
- Forestry Agency of Japan: *Results of Surveys of Distributions of Radioactive Elements in Forest Ecosystems* <<http://www.rinya.maff.go.jp/j/press/kenho/130329.html>> (accessed 13 June 2013) (In Japanese).
- Hashimoto *et al.* Simple models for soil CO<sub>2</sub>, CH<sub>4</sub>, and N<sub>2</sub>O fluxes calibrated using a Bayesian approach and multi-site data. *Ecol. Modell.* **222**, 1283–1292 (2011).
- Ministry of the Environment: *Japan Integrated Biodiversity Information System-fifth survey* <<http://www.biodic.go.jp/english/J-IBIS.html>> (accessed 13 June 2013).
- Wessel, P. & Smith, W. H. F. New, improved version of generic mapping tools released. *Eos, Trans. Am. Geophys. Uni.* **79**, 579 (1998).

## Acknowledgements

The study was supported by FFPRI.

## Author contributions

S.H. designed the study, conducted the simulations with G.S. and wrote the manuscript with input from G.S., I.L., T.M., K.N. and S.K. S.K. provided the observational data. T.M. and K.N. conducted the GIS analyses of the input data.

## Additional information

**Supplementary information** accompanies this paper at <http://www.nature.com/scientificreports>

**Competing financial interests:** The authors declare no competing financial interests.

**How to cite this article:** Hashimoto, S. *et al.* Predicted spatio-temporal dynamics of radiocesium deposited onto forests following the Fukushima nuclear accident. *Sci. Rep.* **3**, 2564; DOI:10.1038/srep02564 (2013).



This work is licensed under a Creative Commons Attribution-NonCommercial-ShareAlike 3.0 Unported license. To view a copy of this license, visit <http://creativecommons.org/licenses/by-nc-sa/3.0>